A model based, anatomy dependent method for ultra-fast creation of primary SPECT projections

Original Article

Faraz Kalantari[1], Hossein Rajabi[1], Mohsen Saghari[2], Alireza Emami Ardekani[2]

[1]Department of Medical Physics, Tarbiat Modares University, Tehran, Iran
[2]Research Institute for Nuclear Medicine, Tehran University of Medical Sciences, Tehran, Iran

(Received 25 August 2011, Revised 14 September 2011, Accepted 22 September 2011)

ABSTRACT

Introduction: Monte Carlo (MC) is the most common method for simulating virtual SPECT projections. It is useful for optimizing procedures, evaluating correction algorithms and more recently image reconstruction as a forward projector in iterative algorithms; however, the main drawback of MC is its long run time. We introduced a model based method considering the effect of body attenuation and imaging system response for fast creation of noise free SPECT projections.
Methods: Collimator detector response (CDR) was modeled by layer by layer blurring of activity phantom using suitable Gaussian functions. Using the attenuation phantom, in each angle, attenuation factor (AF) was calculated for each voxel. This calculated AF is the weight for the emission voxel and states the detection probability of photons that are emitted from that voxel. Finally weighted ray sum of the blurred phantom was driven to create a projection. For the next projection, our phantom was rotated and the procedure was repeated until all projections were acquired.
Results: Root Mean Square error (RMS) between all 60 modelled projection and real MC simulated projections was decreased from 0.58 ± 0.15 using simple Radon to 0.19 ± 0.03 using our suggested model. This value was 0.56 ± 0.16 using blurred Radon without attenuation modelling, and 0.21 ± 0.03 using attenuated Radon without CDR modelling.
Conclusion: Our suggested model that considers the effect of both attenuation and CDR simultaneously results in more accurate analytical projections compared with conventional Radon model. Creation of 60 primary SPECT projections in less than one minute may make this method as a proper alternative for MC simulation. This model can be used as a forward projector during iterative image reconstruction for correction of CDR and attenuation that is necessary for quantitative SPECT.

Keywords: Monte Carlo, SPECT, Projection, Modeling, Attenuation, Collimator detector response

Iran J Nucl Med 2011;19(1):21-29

Corresponding author: Dr. Hossein Rajabi, Department of Medical Physics, Tarbiat Modares University, Tehran, Iran. E-mail: hrajabi@modares.ac.ir

INTRODUCTION

With the advent of high speed computers, Monte Carlo (MC) techniques have become powerful and popular tools in different areas of medical physics. They are extensively used to simulate processes with random nature and to quantify physical parameters that are difficult or impossible to calculate analytically. In particular, many dedicated MC programs have been developed and optimized in the field of nuclear medicine imaging. Source distribution (activity phantom) and attenuation map (attenuation phantom) are the main components of MC simulation. If the behavior of the imaging system can be described by known probability density functions, then the Monte Carlo simulation trace a photon by sampling from these functions using random numbers (1-3). Photons are generated within the activity phantom and are transported by sampling through the attenuation phantom and detection system.

Monte Carlo techniques are extensively used to evaluate the performance of new collimators and scanners in SPECT (4, 5) and PET (6-8), to find optimum imaging conditions and parameters (9), to investigate the strengths and limits of attenuation, scatter and partial volume correction algorithms, since it is possible to obtain a reference image for comparison (10-12) and to reconstruct images using inverse Monte Carlo techniques by computation of the system probability matrix (13-15).

The main drawback of MC is its very long computation time for tracing photons from their emission points to their final detected pixels in projections. There are a number of studies trying to accelerate MC simulation by applying variance reduction techniques such as force detection (16, 17). This method forces every photon to escape through attenuation phantom and finally assigns a suitable weight (regarding the amount of attenuation in photon path) to the detected event. Therefore all photons are detected in the projections. This makes MC more efficient with much higher detection efficiency. The other methods try to model the imaging process to calculate projections analytically. There are also methods that combine both modeling and force detection methods to improve the accuracy of calculated projections. The first and the simplest assumption for creating primary projection from activity distribution is Radon transform. This transform assumes that a pixel value in a projection is the ray sum of the activities in a column in front of it. However, in this assumption, the attenuation of photons inside the objects and non-ideal collimation is ignored. It has been shown that collimator-detector response (CDR) for low energy photons can be accurately modeled by distance dependent Gaussian functions. There are also some methods that consider the effect of attenuation, but neglect the effect of distance dependent collimator blurring.

In this study we introduced a fully analytical model considers the effect of both body attenuation and CDR for very fast creation of noise free SPECT projections. The accuracy of this model was compared with simple Radon transform, attenuated Radon transform without CDR modelling and CDR modelling without attenuation modelling.

METHODS

Digital phantom

To evaluate the performance of our suggested model in a realistic condition, the 4D nonuniform B-spline (NURBS) based cardiac torso (NCAT) phantom was used (18). This phantom precisely models the torso organs and their motions. The NCAT phantom produces the attenuation map and the activity distribution map automatically based on the user defined data (Figure 1). In activity distribution map, ^{99m}Tc activity was considered in myocardium, liver, spleen and other parts of torso (myocardium: liver:

spleen: lung: background 100: 40: 22: 6: 6) based on published data for methoxyisobutyl isonitrile (MIBI) bio-distribution (19). The corresponding attenuation map was created at photon energy of 140 keV. The phantom dimension was 40×40×20 and digitized into 128×128×64 voxel arrays.

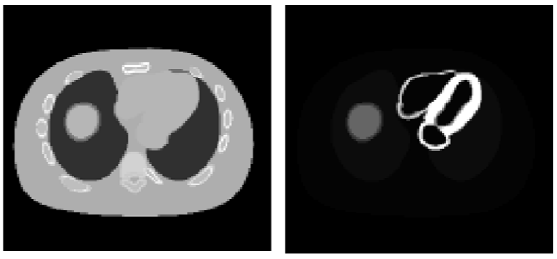

Fig 1. A transaxial slice of NCAT phantom; Activity distribution (right) and its corresponding attenuation map (left)

MC simulation

The Monte Carlo code, SIMIND version 49, was used to create projections from the phantoms (20). A typical SPECT system (Argus, ADAC, USA) with low energy high resolution (LEHR) collimator, 3.4mm intrinsic spatial resolution, 9.7% energy resolution (at 140keV) was modeled in this study. A total number of 64 projections at 128×128 matrix size were acquired in 360 degrees around the phantoms (radius of rotation=30 cm). Since scatter modelling was not aimed in this study, only primary photons were considered to form the projections. Five million photon histories per projection were traced to create almost noise free MC simulated projections. These projections were used as reference images. All of the analytical projections were compared with these reference projections.

Model based projections

Four different mathematical models were applied to create analytical projections from digital phantoms.

Simple Radon transform

Figure 2 illustrates the creation of a 2D projection described by $p(s,n)$ from the 3D activity distribution describes by $f(r,s,n)$ using Radon transform.

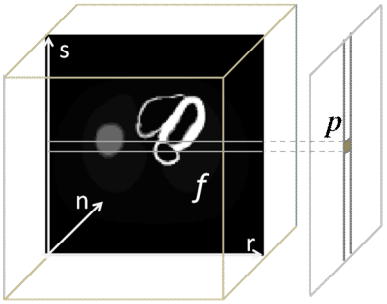

Fig 2. Creation of a 2D projection from the 3D activity distribution using Radon transform. Each pixel value in the projection is equal to the ray sum of activity in front of it.

This model assumes that the total count detected in a pixel, is the simple ray sum of activity in a column placed in front of that pixel. Mathematically, Radon transform can be described by:

$$p(s,n)=\int_0^L f(r,s,n)dr$$

Equation 1

To create an analytical projection using this model, a program was developed in MATLAB R2009b (Mathworks Inc., USA) to calculate the simple ray sum of activity. For the next projection, the activity phantom was rotated in its fixed grid. The procedure was repeated 64 times, until all the analytical projections were created.

Attenuated Radon transform

This model considers the effect of attenuation precisely. Figure 3 illustrates the creation of an attenuated 2D projection described by $p(s,n)$ from the 3D activity

distribution describes by $f(r,s,n)$ using attenuated Radon transform.

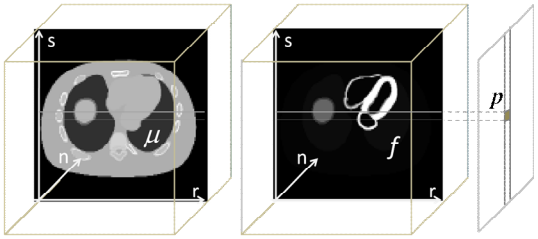

Fig 3. Creation of a projection from the 3D activity distribution using attenuated Radon transform. Each pixel value in the projection is equal to the weighted ray sum of activity in front of it.

The total count detected in a pixel of projection is assumed to be the weighted ray sum of activity in a column of activity in front of it. The weight is determined as the exponential of the sum of the linear attenuation coefficients placed in front of that voxel lie in a path perpendicular to detector, from the emission point to detector. This model can be expressed mathematically by:

$$p(s,n)=\int_0^L f(r,s,n)\exp\left[-\int_r^L \mu(r',s,n)dr'\right]dr$$

Equation 2

Attenuated projections were calculated using a program in MATLAB. For the next projections, both the activity and attenuation phantoms were rotated in its fixed grid. The procedure was repeated until all the attenuated projections were created.

Blurred projections

Modeling of CDR was achieved by layer by layer blurring of our activity phantom using suitable Gaussian functions. To find these Gaussians, the point spread function of system was determined by MC simulation of a point source of activity in different distances from the head of camera. This can be done practically by placing a point source in front of camera head and changing the camera radius to acquire PSFs for different distances. It has been shown that for low energy photons PSFs can be accurately modeled by distance dependent Gaussian functions ($h(r)$) (10, 21). The simple ray sum of this blurred phantom was then calculated to create a blurred projection. This procedure has been shown in figure 4.

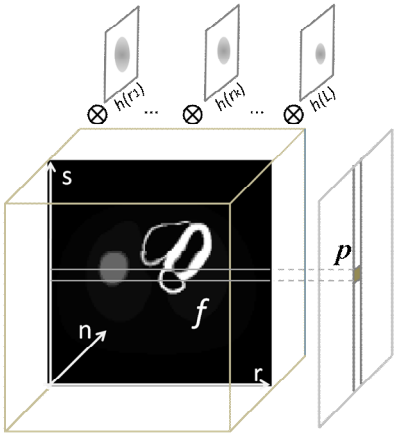

Fig 4. Creation of a blurred projection from the 3D activity distribution; the activity phantom was blurred layer by layer using suitable Gaussian function. The simple ray sum of this blurred phantom was calculated to create a blurred projection.

This model can be expressed mathematically by:

$$p(s,n)=\int_0^L (f(r,s,n)\otimes h(r))dr$$

Equation 3

In the above equation, $h(r)$ stands for distance dependent Gaussian kernels their width varies according to their distance from the face of camera. For the next projections, the activity phantom was rotated in its fixed grid.

Attenuated-blurred projections

This model simultaneously considers the effects of both CDR and attenuation in creation of analytical projections. On the other words, this model combines two previous models to create analytical projections. As described in previous section, the activity phantom was blurred layer by layer using distance dependent Gaussian kernels. The attenuated projections of this blurred phantom were then calculated using attenuated Radon transform. This model can be expressed mathematically by:

$$p(s,n)=\int_0^L \left(f(r,s,n)\otimes h(r)\right)\exp\left[-\int_r^L \mu(r',s,n)dr'\right]dr$$

Equation 4

For the next projections, both the activity and attenuation phantoms were rotated in its fixed grid. The procedure was repeated until all the attenuated projections were created.

Evaluation parameters

Both visual inspection and quantitative comparison was done to evaluate the ability of different methods to model mathematical projections. For visual inspection, four different projections acquired by different methods were shown and compared with reference (MC simulated) projections. To quantitatively evaluate the amount of similarity between each projection (I) and the reference image (I_0), the total count of each projection was first normalized to the total count of reference image and the amount of root mean square (RMS) was then calculated as:

$$RMS=\sqrt{\frac{\sum_{i,j=1}^{n}\left(I_0(i,j)-I(i,j)\right)^2}{n\times n}}$$

Equation 5

The value of n in above equation is 128 for all sets of projections. This helped us to evaluate the relative variation of similarity between reference projection and projections acquired using different mathematical models. Less RMS value means more similarity.

RESULTS

Figure 5 shows four different projections around the NCAT phantom acquired using different methods. These projections consist of the anterior (Ant), left lateral (LL), posterior (Post) and right lateral (RL) acquired using MC simulation (5-a), simple Radon transform (5-b), blurred without attenuation (5-c), attenuated Radon transform (5-d), and our suggested model that simultaneously considers the effect of both CDR and attenuation (5-e).

Figure 6 shows the amount of the RMS for all 60 projections acquired in equally distant angles around the NCAT phantom from anterior to left lateral, posterior, right lateral and anterior again. This value has been shown for all different methods compared to reference projections acquired by MC simulation. This graph shows the strengths and weaknesses of different models in creation of mathematical projections in different angles around the NCAT phantom. There is a significant difference between methods that consider the effect of the attenuation and those neglect the attenuation. There is also a little improvement in our suggested model compared to attenuated Radon that neglects the CDR (Table 1).

DISCUSSION

There are many advantages associated by MC simulation. However the only disadvantage of this simulation method is its long run time to trace each event from its emission point to its final destination. The interest in fully 3D reconstruction approaches spurred the development of fast

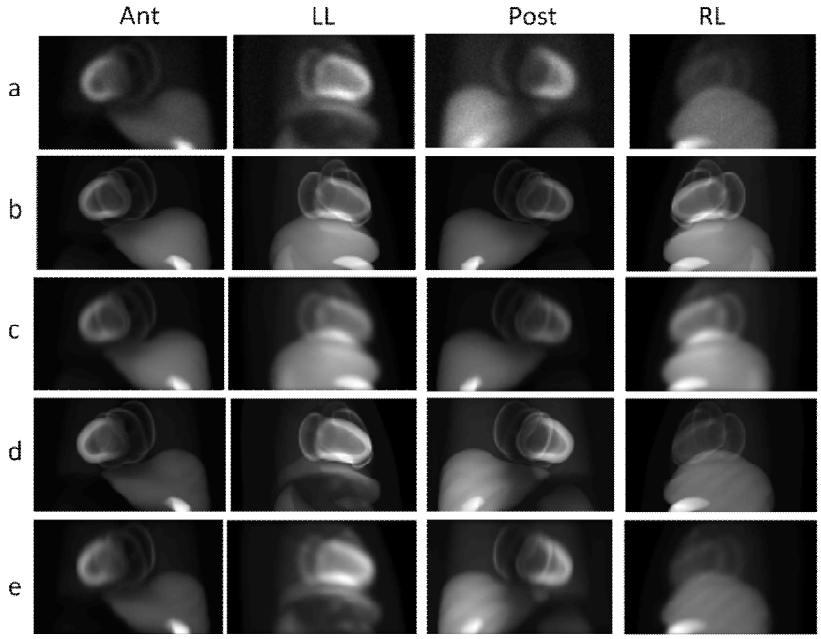

Fig 5. Four different projections acquired from different angles around the NCAT phantom using MC simulation (a), simple Radon transform (b), blurred projections (c), attenuated Radon transform (d) and simultaneous modeling of both attenuation and CDR blurring.

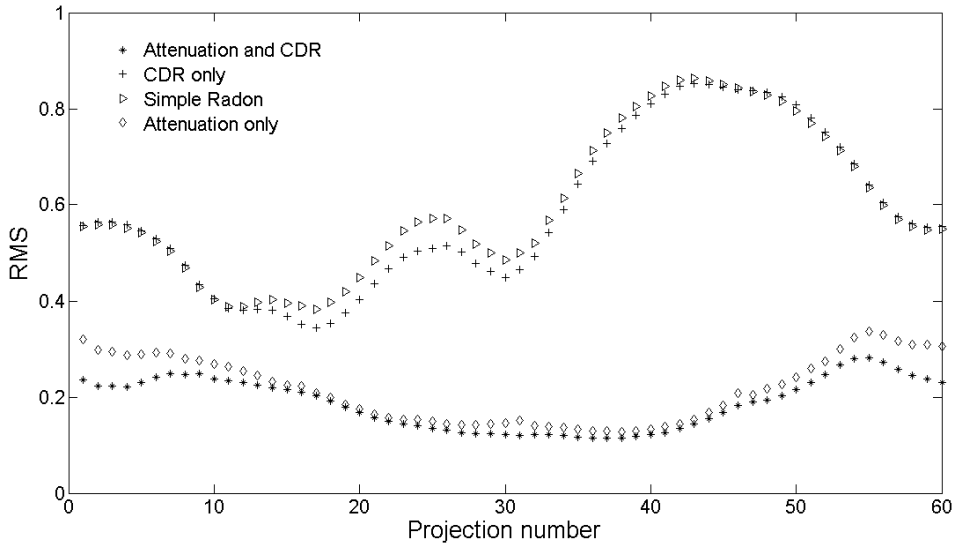

Fig 6. The amount of RMS between analytical projections created by different models and the reference projections acquired by MC simulation.

Table 1. Mean ± standard deviation for RMS between MC simulated and modeled projection for different mathematical models

Applied Model	Simple Radon	Blurred Radon No Attenuation	Attenuated Radon No CDR	Attenuated Radon And CDR
RMS	0.58 ± 0.15	0.56 ± 0.16	0.23 ± 0.04	0.19 ± 0.03

and computationally efficient algorithms capable of obtaining highly accurate projections in clinically acceptable computation times. In this paper we developed a mathematical method for ultra-fast creation of virtual SPECT primary projections considers the effect of both body attenuation and CDR simultaneously. We also applied this model on NCAT phantom with realistic activity distribution. We used a dedicated MC simulator, SIMIND, to create the reference primary projections. We also compared our suggested model with the other conventional models consists of simple Radon transform, attenuated Radon transform and another model considers the effect of CDR but neglects the effect of attenuation. In this research we concentrate on primary photons modelling, because scatters have very complicated behavior and the scatter functions vary from each point to the other point of the body. However there are methods that simplify scatter distribution using simple scatter functions (22-24).

Using our suggested model, creation of 60 noise-free primary projections takes less than one minute. This means that we need less than one second for each projection. This time is considerably less than the run time of any MC simulator for creating a noise-free projection. To have an almost noise-free projection it is necessary to have at least five million detected events in a 128×128 projection. This needs at least 5 million photon tracing in dedicated MC simulator with perfect efficiency that use variance reduction techniques and much more tracing in a real MC simulator that needs much more time (a few minutes to several days) (15).

As shown in figure 5, our suggested model creates projections with higher degree of similarity to the reference projections compared to conventional models. This can be easily seen by visual inspection especially when concentrate on the heart and liver regions. Figure 7 quantitatively confirm our visual inspection. It is clear that RMS values for our suggested model are significantly lower than the conventional models. The other important finding from figure 7 is that the models consider the effect of attenuation, create much better results compared to models that neglect the attenuation. Therefore, this is important to correct for attenuation to have accurate quantitative results. On the other hand, CDR modeling has less effect in myocardial perfusion SPECT. But we should note that this result may be totally different when we scan small objects in which CDR can significantly degrade the quantitative accuracy. The quantitative error due to neglecting attenuation is more noticeable in projections number 25-28 (posterior) and 40-50 (right lateral); this is why myocardial SPECT normally performed from left posterior oblique (LPO) to right anterior oblique (RAO) to avoid posterior and right lateral oblique projections.

CONCLUSION

Our suggested model that considers the effect of both attenuation and CDR simultaneously results in more accurate analytical projections compared with conventional Radon model. Creation of 60 primary SPECT projections in less than one minute may make this method as a proper alternative for MC simulation. This model can be used as a forward projector during 3D iterative image reconstruction for

correction of CDR and attenuation that is necessary for quantitative SPECT.

REFERENCES

1. Andreo P. Monte Carlo techniques in medical radiation physics. Phys Med Biol. 1991 Jul;36(7):861-920.
2. Ljungberg M, Strand SE, King MA. Monte Carlo calculations in nuclear medicine: Applications in diagnostic imaging. IOP Publishing, Bristol, 1998.
3. Zaidi H. Relevance of accurate Monte Carlo modeling in nuclear medical imaging. Med Phys. 1999 Apr;26(4):574-608.
4. Webb S, Binnie DM, Flower MA, Ott RJ. Monte Carlo modelling of the performance of a rotating slit-collimator for improved planar gamma-camera imaging. Phys Med Biol. 1992 May;37(5):1095-1108.
5. Kimiaei S, Ljungberg M, Larsson SA. Evaluation of optimally designed planar-concave collimators in single-photon emission tomography. Eur J Nucl Med. 1997 Nov;24(11):1398-404.
6. Derenzo SE. Monte Carlo calculations of the detection efficiency of NaI(Tl), BGO, CsF, Ge and plastic detectors for 511 keV photons. IEEE Trans Nucl Sci. 1981;28:131-136.
7. Lopes MI, Chepel V, Carvalho JC, Marques RF, Policarpo AJPL. Performance analysis based on a Monte Carlo simulation of a liquid Xenon PET detector. IEEE Trans Nucl Sci. 1995;42:2298-2302.
8. Geramifar P, Ay MR, Zafarghandi MS, Sarkar S, Loudos G, Rahmim A. Investigation of time-of-flight benefits in an LYSO-based PET/CT scanner: A Monte Carlo study using GATE. Nucl Inst Meth Phys Res. 2011;641(1):121-127.
9. Kalantari F, Rajabi H, Yaghoobi N. Optimized energy window configuration for ^{201}Tl imaging. J Nucl Med Technol. 2008 Mar;36(1):36-43.
10. Yokoi T, Shinohara H, Onishi H. Performance evaluation of OSEM reconstruction algorithm incorporating three-dimensional distance-dependent resolution compensation for brain SPECT: a simulation study. Ann Nucl Med. 2002 Feb;16(1):11-8.
11. Narita Y, Eberl S, Iida H, Hutton BF, Braun M, Nakamura T et al. Monte Carlo and experimental evaluation of accuracy and noise properties of two scatter correction methods for SPECT. Phys Med Biol. 1996 Nov;41(11):2481-96.
12. Kalantari F, Rajabi H, Saghar M. Quantification and reduction of attenuation related artifacts in SPET by applying attenuation model during iterative image reconstruction: A Monte Carlo study. Hell J Nucl Med. 2011 Sep;14(3):278-83.
13. Floyd CE, Jaszczak RJ, Coleman RE. Inverse Monte Carlo: a unified reconstruction algorithm for SPECT. IEEE Trans Nucl Sci. 1985;32:779-785.
14. Bowsher JE, Floyd CE Jr. Treatment of Compton scattering in maximum-likelihood, expectation-maximization reconstructions of SPECT images. J Nucl Med. 1991 Jun;32(6):1285-91.
15. Lazaro D, El Bitar Z, Breton V, Hill D, Buvat I. Fully 3D Monte Carlo reconstruction in SPECT: a feasibility study. Phys Med Biol. 2005 Aug 21;50(16):3739-54.
16. De Jong HWAM, Slijpen ETP, Beekman FJ. Acceleration of Monte Carlo SPECT simulation using convolution-based forced detection. IEEE Trans Nucl Sci. 2001; 48:58-64.
17. Haynor DR, Harrison RL, Lewellen TK. The use of importance sampling techniques to improve the efficiency of photon tracking in emission tomography simulations. Med Phys. 1991 Sep-Oct;18(5):990-1001.
18. Segars WP, Lalush DS, Tsui BMW. Modeling respiratory mechanics in the MCAT and splinebased MCAT phantoms. IEEE Trans Nucl Sci. 2001;48:89-97.
19. Wackers FJ, Berman DS, Maddahi J, Watson DD, Beller GA, Strauss HW et al. Technetium-99m hexakis 2-methoxyisobutyl isonitrile: human biodistribution, dosimetry, safety, and preliminary comparison to thallium-201 for myocardial perfusion imaging. J Nucl Med. 1989 Mar;30(3):301-11.

20. Ljungberg M, Strand SE. A Monte Carlo program for the simulation of scintillation camera characteristics. Comput Methods Programs Biomed. 1989 Aug;29(4):257-72.

21. Beekman FJ, Eijkman EGJ, Viergever MA, Borm GF, Slijpen ETP. Object shape dependent PSF model for SPECT imaging. IEEE Trans Nucl Sci. 1993;40(1):31-9.

22. Axelsson B, Msaki P, Israelsson A. Subtraction of Compton-scattered photons in single-photon emission computerized tomography. J Nucl Med. 1984 Apr;25(4):490-4.

23. Frey EC, Tsui BMW. A new method for modeling the spatially-variant, object-dependent scatter response function in SPECT. IEEE Nucl Sci Symp and Med Imaging Conf. 1996;2:1082-6.

24. Beekman FJ, den Harder JM, Viergever MA, van Rijk PP. SPECT scatter modelling in non-uniform attenuating objects. Phys Med Biol. 1997 Jun;42(6):1133-42.

25. Beekman FJ, de Jong HW, van Geloven S. Efficient fully 3-D iterative SPECT reconstruction with Monte Carlo-based scatter compensation. IEEE Trans Med Imaging. 2002 Aug;21(8):867-77.